Reactive Uptake of Ozone by Oleic Acid Aerosol Particles: Application of Single-Particle Mass Spectrometry to Heterogeneous Reaction Kinetics

Geoffrey D. Smith,[†] Ephraim Woods, III,[‡] Cindy L. DeForest,[§] Tomas Baer,* and Roger E. Miller*

Department of Chemistry, University of North Carolina, Chapel Hill, North Carolina 27599-3290

Received: February 26, 2002; In Final Form: June 18, 2002

The technique of single-particle mass spectrometry has been coupled to a reaction flow tube to measure the uptake coefficient, γ, of ozone (O_3) by oleic acid (9-octadecenoic acid) aerosol particles. The reaction was followed by monitoring the decrease of oleic acid in the size-selected particles as a function of O_3 exposure. The reactive uptake coefficient is found to depend on the size of the particle, with γ_{meas} ranging from $(7.3 \pm 1.5) \times 10^{-3}$ to $(0.99 \pm 0.09) \times 10^{-3}$ for particles ranging in radius from 680 nm to 2.45 μm. It is suggested that the decrease in γ_{meas} with increasing particle size results from the reaction being limited by the diffusion of oleic acid within the particle, and based on our measurements we estimate the value of γ to be $(5.8-9.8) \times 10^{-3}$ for particles that are not limited by oleic acid diffusion. A reaction model that includes simultaneous diffusion and reaction of both O_3 and oleic acid is developed and used to fit the observed rates of reaction. Solutions obtained from this model indicate that oleic acid must diffuse within the particle more slowly than is predicted by the measured oleic acid self-diffusion constant.[1] It is proposed that this oleic acid-diffusion-limited uptake is attributable to the ozonolysis reaction products. Furthermore, these experiments demonstrate that it is not always possible to describe heterogeneous uptake by a model that decouples all relevant processes, including reaction and diffusion. Finally, the possible implications that these findings have for the role of particle morphology in the reaction of gas-phase species with atmospheric aerosols are discussed.

Introduction

Organic aerosols and aerosols containing significant quantities of organic species are common throughout the troposphere.[2−4] Nonurban aerosols contain a variety of organic species of biogenic origin including alkanes, alkenes, fatty acids, alcohols, and aromatics.[5−8] In urban areas, particles composed of organics can also be emitted directly into the atmosphere from various sources including automobile exhaust, natural gas combustion, wood and cigarette smoke, and cooking exhaust.[9,10] Particles can also be formed or increase in size through the photochemical oxidation of organic species to create multifunctional organics which often have vapor pressures low enough that they exist primarily in the condensed phase. These organic aerosols may significantly affect the climate by acting as cloud condensation nuclei, which may consequently affect cloud albedo.[7] Organic species may also play a role in the chemistry occurring within these aerosols as well as affect the atmospheric budgets of gas-phase species, including important oxidizing species such as O_3 and HO_2.[11,12]

Ozone is one of the most important oxidants in the troposphere, and it is the photolytic precursor to the hydroxyl radical that is primarily responsible for the oxidation of hydrocarbons in the atmosphere. Ozone is also a significant component of photochemical smog and can lead to adverse effects on human respiratory health as well as on vegetation. Organic species, especially unsaturated hydrocarbons, are known to react with O_3 in both the gas phase and in solution. Reaction rates and product yields for reactions between O_3 and unsaturated compounds in the gas phase have been measured, but these reactions are fairly inefficient, with second-order rate constants ranging in value from 10^{-18} cm^3 molecule^{-1} s^{-1} to 10^{-14} cm^3 molecule^{-1} s^{-1}.[7] On the other hand, it has been shown that heterogeneous reactions of O_3 with unsaturated species in solution can be efficient[13] and may have significant implications for the loss of O_3 in the troposphere and on the identities of the condensed-phase species in aerosols.

Many previous studies measuring gas-phase uptake by condensed-phase samples have been conducted by monitoring the loss of the gas-phase species using Knudsen cell reactors[14] and coated-wall flow tubes.[15,16] With these techniques, nonreactive uptake (such as physical adsorption) cannot be distinguished from reactive uptake. In addition, when uptake by a liquid sample is monitored, reaction with vapor above the liquid cannot be distinguished from reaction in the bulk of the liquid. A notable exception to these techniques is the recent work of Worsnop and co-workers, in which they used a thermal desorption-EI aerosol mass spectrometer to monitor reactive uptake of a gas-phase species from the perspective of the particle.[17]

In the present work, a dual-laser single-particle mass spectrometer is used to follow the progress of a reaction by monitoring the concentration of the condensed-phase species. The use of separate vaporization and ionization lasers results in less fragmentation than with other methods, making the approach particularly well suited to the study of reactions with organic species.[18] Additionally, the dual laser approach makes

* Corresponding authors.
[†] Present address: University of Georgia, Department of Chemistry, Chemistry Bldg., Athens, GA 30602.
[‡] Present address: Colgate University, Department of Chemistry, 13 Oak Dr., Hamilton, NY 13346.
[§] Present address: Davidson College, Department of Chemistry, Box 7120, Davidson, NC 28035.

10.1021/jp020527t CCC: $22.00
Published on Web 08/02/2002

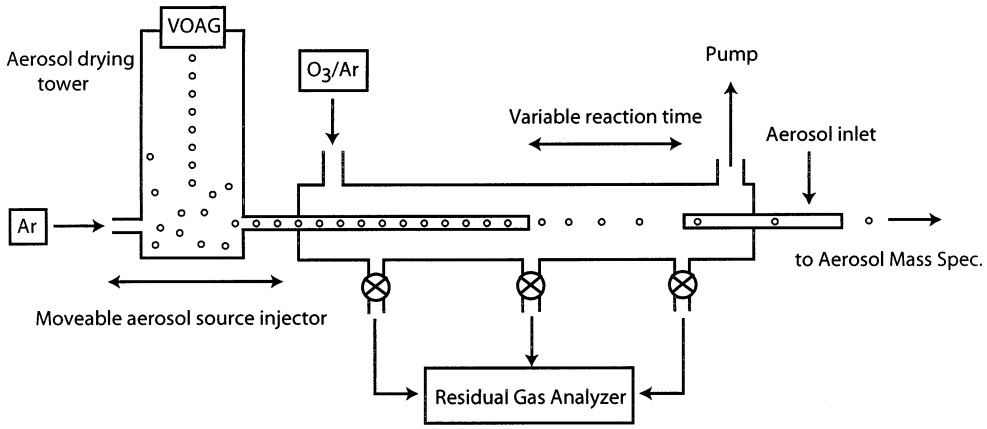

Figure 1. Schematic of aerosol flow tube. Oleic acid particles are created with the VOAG and enter the flow tube through the moveable aerosol injector. Ozone passes through the UV absorption cell into the rear of the flow tube. The reaction time between the O_3 and the oleic acid particles is varied by moving the position of the aerosol injector. Particles exit the flow tube and are sampled by the aerosol mass spectrometer.

it is possible to gently probe the identities of the species present in the condensed phase following reaction and may offer insight into the mechanism of the reaction. Furthermore, since many heterogeneous reactions occur near the surface, the uptake kinetics may be limited by diffusion of the reactants within the particle to the surface region. Measuring the uptake as a function of particle size allows us to assess the importance of this diffusion.

We have coupled an aerosol flow tube to our dual-laser single-particle mass spectrometer to measure the reactive uptake of O_3 by particles of a particular unsaturated species, oleic acid. Oleic acid is found in many meats and cooking oils and is, in fact, the primary unsaturated species in olive oil. Oleic acid has been measured in tropospheric aerosols at concentrations of $\sim$1 ng m^{-3},[10] and in the present experiments it serves as a suitable representative of many unsaturated species typically found in these aerosols. In addition, the kinetics of this reaction have been studied recently by Worsnop and co-workers,[17] providing a useful comparison for this novel technique.

Experiment

Aerosol Flow Tube. The apparatus used in these experiments consists of an aerosol flow tube (Figure 1) and a dual-laser single-particle mass spectrometer, which is described in detail in our previous work.[18,19] A vibrating orifice aerosol generator (VOAG) (TSI, Inc.) is used to create a monodisperse stream of droplets containing oleic acid (Aldrich, CAS# 112-80-1) and 2-propanol. The droplets are directed into an acrylic drying tower by an argon flow (Air Products, research grade) of 2 STP L min^{-1}, where the 2-propanol from the droplets evaporates, thereby generating a monodisperse aerosol of pure oleic acid. Another 2 STP L min^{-1} flow of argon sweeps the particles out of the tower into a one-meter long, 1/4 in. o.d. Pyrex injector tube, which enters the 1-m long, 1 in. i.d. Pyrex reaction flow tube from the rear. The drying tower and injector are moveable along an optical rail, allowing for a variable injection position of the aerosols along the length of the flow tube.

Ozone is generated by flowing O_2 (Air Products, research grade) through an ozonizer (Pacific Ozone Technology, model L11), and it is stored in a glass trap containing silica gel and cooled to 196 K with a 2-propanol/dry ice bath. Ozone is carried from the trap by a flow of argon (10$-$60 STP cm^3 min^{-1}), passes through an absorption cell where the absolute concentration is measured, is diluted by another flow of argon (500 STP cm^3 min^{-1}), and then enters the rear of the flow tube. The 10-cm long cell is constructed from 1/2 in. o.d. quartz with 1/4 in. o.d. inlets and outlets for the O_3 flow. Light from a pen-ray Hg lamp (VWR Scientific), selected with a notch filter (Melles Griot, $\lambda = 254$ nm $\pm$ 5 nm), passes through the length of the cell and is then detected with a calibrated, UV-sensitive photodiode (Edmund Scientific). The concentration of the O_3 flowing through the cell is determined from the measured absorption, the known path length, and the known cross section (1.169×10^{-17} cm^2 molecule^{-1} at $\lambda = 254$ nm[20]). The concentration of O_3 in the flow tube (6×10^{-6} to 1×10^{-4} atm) is calculated from the concentration measured in the cell and the known gas flows regulated with calibrated mass flow controllers (MKS Instruments). The concentration of O_3 is also monitored with a residual gas analyzer (RGA) (Stanford Research Systems), sampling gas through one of three ports located along the length of the flow tube.

The reaction of O_3 with pure oleic acid particles is studied by monitoring the concentration of oleic acid within the particles as a function of O_3 exposure using our single-particle mass spectrometer. The O_3 exposure ($P_{O_3}t$) is varied by adjusting the reaction time with a fixed O_3 partial pressure. The residual gas analyzer is used to monitor the partial pressure of O_3 in the flow tube both with and without particles present. Stable O_2^+ and O_3^+ signals from the residual gas analyzer indicate that the partial pressure of O_3 is uniform throughout the flow tube and that the number density of particles is not great enough to deplete it.

The reaction time is varied by moving the position of the aerosol injector within the flow tube. A "turbulizer" placed coaxially with the injector and located 3 cm from the exit end serves to hold the injector in place and introduce turbulence downstream of the injector. The flow velocities of the flow tube flow (1.6 cm s^{-1}) and the injector flow (530 cm s^{-1}) are sufficiently different so that turbulent flow develops past the exit of the injector. However, the turbulizer enhances mixing of the O_3 flow with the flow of particles exiting the injector to ensure that there is no time delay due to diffusive mixing of the O_3 (which would require $\sim$0.5 s).

The residence time of the particles is calculated as a function of injector position within the flow tube by measuring the time delay between the initiation of their creation with the VOAG and their detection via the light scattering stations in the aerosol mass spectrometer. This total time represents the time required for the particles to travel through the drying tower, the moveable injector, the flow tube, and the aerosol inlet. Then, the time

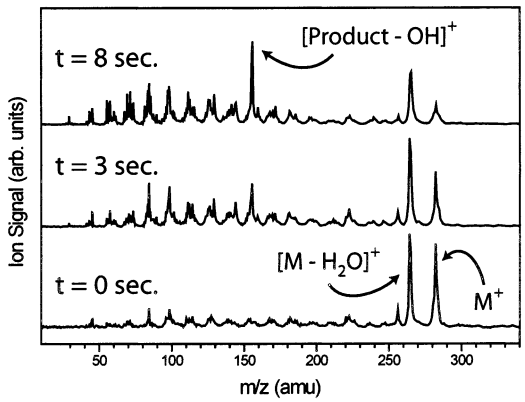

Figure 2. Mass spectra of oleic acid particles of radius 2.45 μm with $P_{O_3} = 1.3 \times 10^{-4}$ atm and reaction times of 0, 3, and 8 s.

required for the particles to travel just through the drying tower and the moveable injector (measured separately) is subtracted from the total time, thereby allowing a direct correlation to be made between the position of the injector within the flow tube and the particle residence time in the flow tube. The residence times measured in this manner are found to approximate closely the times predicted by the bulk flow velocity of the gas, and all decay data presented here are analyzed with the measured times.

Single-Particle Mass Spectrometer. Aerosol particles from the flow tube are sampled into the single-particle mass spectrometer through an 18-cm long, 1/4 in. o.d. stainless steel inlet terminated by a 100-μm i.d. flow-limiting orifice. After passing through this orifice the particles enter a 20-cm long aerodynamic lens,[21−23] which focuses them along a well-defined axis and greatly improves the efficiency with which they are detected. The focused particles are then accelerated through two stages of differential pumping, after which they pass through two 532-nm diode lasers separated by 10 cm. The velocities of the particles are calculated from the time difference between the scattering signals, and a digital timing circuit triggers the pulsed lasers to vaporize and ionize the particles when they reach the mass spectrometer. The measured velocities are also used to calculate the aerodynamic diameter of each particle.

A two-laser scheme is employed consisting of a pulsed TEA−CO_2 laser (Lumonics) for vaporization of the particle and a pulsed vacuum−ultraviolet (VUV) laser for ionization of the resulting gas plume. The typical CO_2 laser energies range from 30 to 65 mJ/pulse, with an estimated focal spot size of approximately 1 mm^2. After a variable delay of 2−30 μs, a 118.5 nm pulse, created by frequency-tripling the 355 nm output of a Nd:YAG laser (Continuum) in a Xe/Ar gas cell, ionizes the vapor plume. The resulting ions are analyzed with the time-of-flight mass spectrometer.

Results

Mass Spectra of Reacted Particles. The soft vaporization and ionization of the two-laser technique allow the detection of oleic acid as its parent ion (M^+, $m/z = 282$), and from this feature in the mass spectrum (Figure 2) the concentration of oleic acid within each particle can be measured. The parent ion at $m/z = 282$ (M^+) accounts for approximately 15% of the entire ion signal (see lowest spectrum in Figure 2), indicating much less fragmentation than with electron impact ionization, which usually results in less than 1% of the ion signal at $m/z = 282$.[17] As the O_3 exposure time increases (upper spectra in Figure 2), the peak at $m/z = 282$ decreases in intensity and a peak at $m/z = 155$ grows proportionally. Figure 3 illustrates these trends

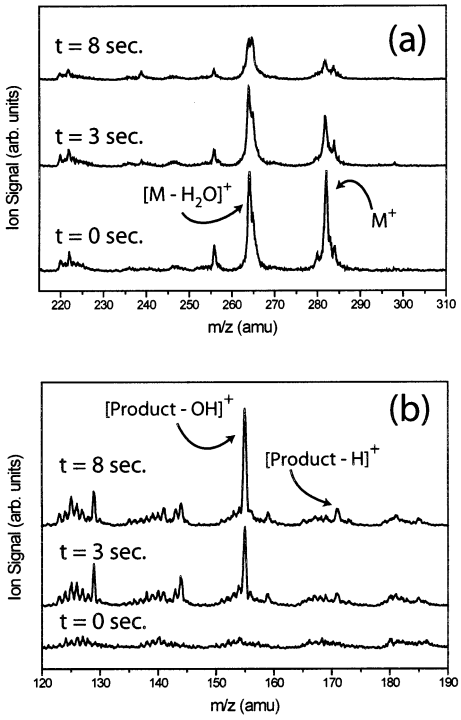

Figure 3. Mass spectra digitized at high resolution for particles of radius 2.45 μm with $P_{O_3} = 1.3 \times 10^{-4}$ atm and reaction times of 0, 3, and 8 s: (a) high-mass peaks including molecular ion of oleic acid (M^+) at $m/z = 282$, (b) low-mass peaks showing emergence of peaks at $m/z = 171$ and $m/z = 155$.

with spectra digitized at higher resolution. These spectra, with >1 amu resolution at $m/z = 282$, were used in analysis of the data to ensure that this peak could be distinguished from neighboring peaks, such as the unsaturated acid impurity at $m/z = 284$.

The ozonolysis of alkenes has been studied in both the gas phase and the condensed phase, and the identities and fates of some of the products from the reactions have been characterized.[11,13,24,25] The mechanism of the ozonolysis of oleic acid is not expected to differ significantly from that of alkenes, as the double bond in oleic acid is located in the middle of the long molecule and is therefore relatively isolated from the carboxylic acid group. It is known that the initial step in ozonolysis reactions is the addition of the ozone across the double bond of the alkene forming the primary ozonide (see Figure 4). This primary ozonide is unstable, and the C−C bond breaks forming two possible pairs of fragments depending on which O−O bond breaks (also shown in Figure 4). In both cases, an aldehyde and a Criegee intermediate are formed. In general, the Criegee intermediate can decompose, be stabilized, or react with an aldehyde fragment to form a secondary ozonide. Thus, a number of primary and secondary products can be formed.

In the spectra shown in Figure 3b, the growth of a feature at $m/z = 155$ can be seen with ozonolysis reaction times of 3 s and 8 s. Other, smaller peaks that appear upon exposure to O_3 are also evident in the spectra. In particular, peaks at $m/z = 125$, 129, 141, 143, 144, 159, and 171 all grow slightly with reaction. The mechanism outlined in Figure 4 reveals possible assignments for these peaks, with the mass-to-charge ratios of experimentally observed peaks underlined. The largest peak in the spectrum, at $m/z = 155$, and the peak at $m/z = 171$ may represent fragments from one of the ozonolysis products, 9-oxononanoic acid ($m/z = 172$). In particular, the peak at $m/z = 171$ could be the H-loss fragment from 9-oxononanoic acid,

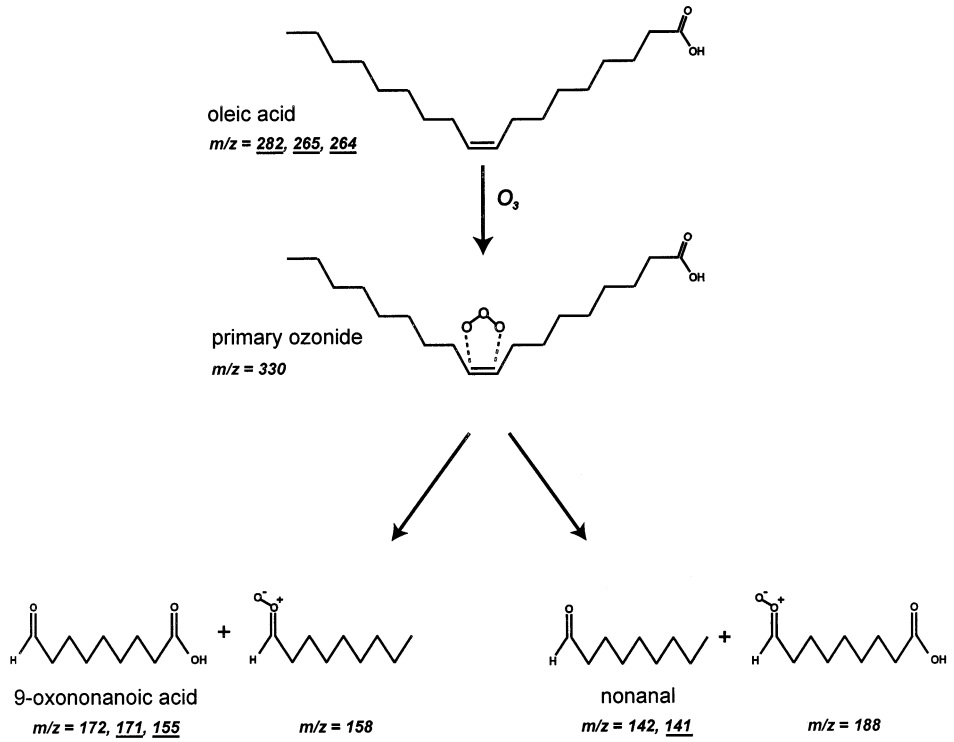

Figure 4. Mechanism for ozonolysis of oleic acid. The mass-to-charge ratios for each species (and associated fragments) are indicated with peaks identified in the spectra of oleic acid particles underlined.

and that at $m/z = 155$ may be the OH-loss fragment from the same product. Interestingly, these same two peaks represented the majority of the product features observed in the study of the reaction of O_3 with oleic acid particles conducted by Ziemann and co-workers using thermal desorption particle beam mass spectrometry.[26] The feature at $m/z = 141$ could be attributed to the H-loss fragment of the nonanal product ($m/z = 142$), which has been observed by Rudich and co-workers in the gas phase in a coated-wall flow tube study of the reaction of O_3 with oleic acid.[27] These assignments are not definitive, however, and the peaks at $m/z = 141$, 155 and 171 could also be attributed to fragments of product species, including secondary ozonides. The other peaks are more difficult to assign to particular ozonolysis products, although their growth is clearly correlated with the increasing exposure to O_3. In particular, lower-mass fragments (including peaks at $m/z = 29$, 43, 57, 70, 82, and 97), which are observed in the spectra of reacted oleic acid particles (shown in Figure 2), also appear in electron-impact spectra of the nonanal ozonolysis product.[28]

Reactive Uptake Model. Though reactive uptake by a condensed phase is typically described in terms of the loss of a gas-phase species, Worsnop and co-workers have shown that it is also possible to interpret the uptake in terms of the loss of a species in the bulk.[17] In the reaction of O_3 with oleic acid, the rate of change of the oleic acid concentration, [Oleic], can be expressed in terms of the reactive O_3 uptake coefficient:

$$\frac{\mathrm{d[Oleic]}}{\mathrm{d}t} = -\gamma\left(\frac{P_{O_3}\bar{c}}{4RT}\right)\frac{S_A}{V} \qquad (1)$$

where γ is the probability that an O_3 molecule colliding with the particle will react either at the surface or in the bulk of the particle. Because γ is a function of [Oleic], the functional form of γ must be known before eq 1 can be solved for [Oleic] as a function of time. The term in parentheses represents the O_3-particle collision rate (mol cm^{-2} s^{-1}), with P_{O_3} the partial pressure of O_3 (in atm), $\bar{c}$ the mean kinetic speed of O_3 molecules in the gas phase (3.6×10^4 cm s^{-1}), R the gas constant (0.082 atm K^{-1} M^{-1}), and T the temperature (298 K). The factor S_A/V ($= 3/a$, where a is the particle radius) is the ratio of the surface area to the volume and normalizes the rate of O_3 uptake to the volume of the particle.

There are many processes that can limit the rate at which a gas-phase species is taken up by a particle. These processes include: gas-phase diffusion to the particle, accommodation at the surface of the particle, reaction on the surface of the particle, incorporation into the bulk of the particle, and reaction within the bulk of the particle.[29,30] The aggregate of these processes can be represented by a set of coupled partial differential equations in the concentrations of the species of interest, with appropriate boundary conditions at the interfaces. Analytical solutions to these equations have been obtained for certain limiting cases.[31−33]

A convenient simplification that is often made in interpreting the interaction of gas-phase species with heterogeneous systems is the use of an electric circuit resistance model.[30,34,35] In this model, each of the processes listed above is considered to be independent of, or decoupled from, all other processes. Each process is represented as an individual conductance (Γ) which is normalized to the gas-particle collision rate and is therefore unitless. This formulation is useful because the individual resistances ($1/\Gamma$) can be combined in series or in parallel to represent the overall uptake coefficient (γ) of the gas-phase species.[35,36] Many experimental studies have utilized this and similar formulations to relate the measured uptake (γ_{meas}) of a gas-phase species by a bulk sample to the reaction probability (Γ_{rxn}) within the sample.[37−39]

We make use of this resistance model to interpret the reactive uptake of O_3 by oleic acid in the present experiments. The limiting loss process for O_3 is reaction with oleic acid, either in the bulk or on the surface, and the net uptake of O_3 by the oleic acid particle is the sum of the uptake due to reaction at

the surface (Γ_{surf}) and the uptake due to reaction in the bulk (Γ_{rxn})

$$\gamma = \Gamma_{rxn} + \Gamma_{surf} \tag{2}$$

It is possible that O_3 could be reacting at both the surface and in the bulk, and thus the measured rate represents both Γ_{surf} and Γ_{rxn}. However, these processes are not coupled to one another as long as the concentration of O_3 at the surface is not significantly affected by either process. The following treatment will utilize analytical expressions for the uptake coefficient to derive expressions for the oleic acid concentration as a function of time in the two limits: Case 1, where Γ_{surf} is negligible compared to Γ_{rxn} and therefore $\gamma_{meas} = \Gamma_{rxn}$; and Case 2, where Γ_{rxn} is negligible compared to Γ_{surf} and therefore $\gamma_{meas} = \Gamma_{surf}$. These expressions can then be used to fit the oleic acid concentration decays measured in the present experiments.

Case 1: Reactive Uptake Dominated by Reaction in the Bulk ($\gamma_{meas} = \Gamma_{rxn}$). The rate of change of the O_3 concentration within the particle can be described by a differential equation including diffusion of O_3 (in the particle) and reactive loss:

$$\frac{\partial[O_3]}{\partial t} = D\nabla^2[O_3] - k[O_3] \tag{3}$$

Here, D is the diffusion coefficient for O_3 in oleic acid (cm^2 s^{-1}) and k ($= k_2[\text{Oleic}]$) is the first-order rate coefficient (s^{-1}) for the reaction of O_3 with oleic acid. This differential equation can be solved analytically if two common assumptions are made: (1) that the concentration of oleic acid is uniform throughout the particle, i.e., oleic acid diffusion is fast, and (2) $[O_3]$ is in steady state, i.e., $d[O_3]/dt = 0$. The derivation of the solutions with these assumptions is given in Appendix I. The consequences of making these assumptions will be discussed in detail in a later section.

With these assumptions, eq 3 can be solved to yield the steady-state O_3 concentration as a function of position within the particle. From this solution, the flux of O_3 into the particle can be calculated. Normalizing this flux to the O_3 particle collision rate yields the reactive uptake coefficient (derivation in Appendix I):

$$\Gamma_{rxn} = \frac{\text{flux}_{surf}}{P_{O_3}\bar{c}/4RT} = \frac{4HRT}{\bar{c}}\frac{D}{\ell}(\coth(a/\ell) - \ell/a) \tag{4}$$

where H is the Henry's Law solubility constant of O_3 in oleic acid ($M\ atm^{-1}$) and a is the radius of the particle. The parameter ℓ is often referred to as the "diffuso-reactive length," and it represents the characteristic distance that an O_3 molecule diffuses before it reacts, namely:

$$\ell = \sqrt{\frac{D}{k_2[\text{Oleic}]}} \tag{5}$$

In this experiment, $D \approx 1 \times 10^{-5}\ cm^2\ s^{-1}$ (estimated based on the diffusion of O_2 in a variety of organic solvents),[40] $k_2 = 1 \times 10^6\ M^{-1}\ s^{-1}$,[41] and $[\text{Oleic}]_0 = 3.16$ M,[42] yielding a value of $\ell \sim 20$ nm. This distance is much smaller than the radius of even the smallest particles used in these experiments (680 nm). This large difference leads to a convenient simplification of eq 4 and is discussed below as Case 1b.

The above expression for Γ_{rxn} (eq 4) can be substituted for γ in eq 1, resulting in a differential equation in [Oleic]. The solutions to this equation can be fit to the observed [Oleic] decays to yield a value for γ_{meas}. Although the differential equation cannot be solved analytically to obtain a solution for [Oleic], it can be solved numerically with knowledge of P_{O_3}, H, D, k_2, and a. Alternatively, analytical solutions can be found for two limiting cases of the diffuso-reactive length, ℓ. Derivations for the solutions for these cases are given in Appendix II.

Case 1a: Fast Diffusion of O_3 Throughout the Particle ($\ell > a$). In this case the rate of reaction will not be limited by O_3 diffusion, such that

$$[\text{Oleic}] = [\text{Oleic}]_0 \exp(-P_{O_3}Hk_2t) \tag{6}$$

$$\gamma = \frac{4HRT}{\bar{c}}\frac{a}{3}k_2[\text{Oleic}] \tag{7}$$

This case is clearly not valid for the experiments described here, given that $\ell \sim 20$ nm and a is at least 680 nm.

Case 1b: Reaction of O_3 Near the Surface of the Particle ($\ell < a/20$). This case is often referred to as the "diffusion-limited" case because the rate of reaction depends on the rate of O_3 diffusion (and γ therefore depends on D). This case is applicable for all particle sizes used in the present experiments. For this case eq 1 can be solved to obtain

$$\sqrt{[\text{Oleic}]} = \sqrt{[\text{Oleic}]_0} - \frac{3P_{O_3}H\sqrt{Dk_2}}{2a}t \tag{8}$$

$$\gamma = \frac{4HRT}{\bar{c}}\sqrt{Dk_2}\sqrt{[\text{Oleic}]} \tag{9}$$

Case 2: Reactive Uptake Dominated by Reaction at the Surface ($\gamma_{meas} = \Gamma_{surf}$). The reaction of O_3 with oleic acid at the surface of the particle can be written as a second-order loss process, similar to the formulation of Worsnop et al.:[43]

$$\begin{aligned}\frac{d[\text{Oleic}]_{surf}}{dt} &= -k_2^{surf}[O_3]_{surf}[\text{Oleic}]_{surf} \\ &= -k_2^{surf}(P_{O_3}H\delta)([\text{Oleic}]\delta)\end{aligned} \tag{10}$$

where the surface concentration of O_3, $[O_3]_{surf}$ (mol cm^{-2}), is approximated as the product of the Henry's Law equilibrium value, $H \cdot P_{O_3}$, and the depth of the surface layer, δ. Likewise, the concentration of oleic acid at the surface, $[\text{Oleic}]_{surf}$ (mol cm^{-2}) is also approximated as the product of [Oleic] and δ. The second-order rate coefficient, k_2^{surf} ($cm^2\ mol^{-1}\ s^{-1}$), is specific to the surface of the particle and is different from the bulk rate coefficient, k_2.

An expression for the reactive uptake coefficient at the surface is obtained by normalizing the rate in eq 10 by the gas-particle collision rate:

$$\Gamma_{surf} = \frac{-\frac{d[\text{Oleic}]_{surf}}{dt}}{P_{O_3}\bar{c}/4RT} = \frac{4HRT}{\bar{c}}\delta^2 k_2^{surf}[\text{Oleic}] \tag{11}$$

An expression for the rate of change of [Oleic] with time can be found by substituting eq 11 in eq 1 and solving for [Oleic]:

$$[\text{Oleic}] = [\text{Oleic}]_0 \exp\left(-\frac{3\delta^2}{a}P_{O_3}Hk_2^{surf}t\right) \tag{12}$$

Since the functional forms of the solutions for Cases 1a, 1b, and 2 are different, the shapes of the measured [Oleic] decays should allow us to identify the operative mechanism. Although

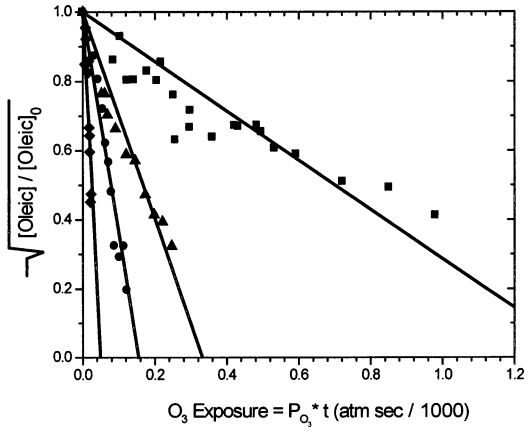

Figure 5. Oleic acid decay profiles as measured with the single-particle mass spectrometer for four particle sizes: ◆ 680 nm, ● 1.38 μm, ▲ 1.86 μm, ■ 2.45 μm. Though linear fits can be made to each decay independently, no single set of parameters (H, D, and k_2) can fit all of the data simultaneously.

Case 1a and Case 2 both yield exponential functions, the solution for Case 1a does not depend on the particle radius, a, whereas the solution for Case 2 does. Both Case 1b and Case 2 depend on the particle size, but they differ in their functional forms (exponential vs square root).

Measurement of Oleic Acid Reaction Kinetics. The concentration of oleic acid in the particles is measured as a function of O_3 exposure ($P_{O_3}t$) for four different particle sizes ranging in radius from 680 nm to 2.45 μm. The oleic acid concentration in the particles is measured as the integrated signal of the oleic acid parent peak ($m/z = 282$) normalized to the signal in the absence of O_3 and is obtained by averaging spectra for 100−200 particles per reaction time. The decay profiles are then fit to each of the two possible solutions identified above, namely the square root decay of Case 1b ($\ell < a/20$) and the exponential decay of Case 2 (surface reaction). Both cases fit the data approximately, although the square root (Case 1b) is better than the exponential (Case 2) when the data for all of the particle sizes are considered. Of course, it is possible that O_3 reacts at both the surface and in the bulk of the particle, but it is difficult to estimate the relative contributions of the two cases without knowledge of the values of k_2, k_2^{surf}, H, and D. Therefore, we assume that one or the other of these processes dominates the reactive uptake, and we believe that the data are better represented by a bulk reaction (Figure 5).

Each of the decay profiles in Figure 5 can be fit to the solution obtained for Case 1b:

$$\frac{\sqrt{[\text{Oleic}]}}{\sqrt{[\text{Oleic}]_0}} = 1 - \frac{3}{2a\sqrt{[\text{Oleic}]_0}}(H\sqrt{Dk_2})(P_{O_3}t) \qquad (13)$$

where the function is expressed as a fractional decay in the oleic acid signal. Values for the quantity $H\sqrt{Dk_2}$ are obtained from the slopes of the linear fits in Figure 5 since the values of a, P_{O_3} and $[\text{Oleic}]_0$ are known for all of the experiments. This quantity can then be replaced in eq 9 to obtain a value for γ_{meas}, the uptake coefficient for pure oleic acid:

$$\gamma_{meas} = \Gamma_{rxn} = \frac{4HRT}{\bar{c}}\sqrt{Dk_2}\sqrt{[\text{Oleic}]_0} \qquad (14)$$

In this way, the value of γ_{meas} is determined from the oleic acid decay profiles without the need for direct measurement of the individual quantities, H, D, and k_2.

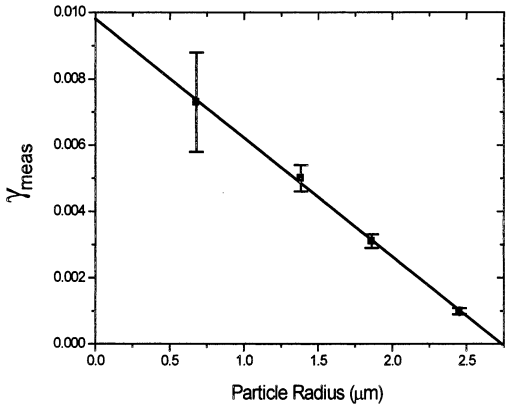

Figure 6. Size dependence in the measured reactive uptake coefficients. No size dependence is predicted by the applicable uptake model (Case 1b).

The value of the reactive uptake coefficient depends on the concentration of oleic acid in the particle, and eq 14 therefore represents the probability of reactive uptake by a pure oleic acid particle. In this expression for γ_{meas} there is no explicit size dependence, and the values calculated for each of the four particle sizes used in these experiments should be identical. However, a plot of γ_{meas} vs particle radius (Figure 6) demonstrates a distinct size dependence in the uptake coefficient. In fact, the observed uptake coefficient decreases linearly with particle size. Though linear fits can be made independently for each of the decays in Figure 5, there is no single set of parameters (H, D, and k_2) that will allow all four sets to be fit simultaneously. Even if the possibility that the data are described by a surface reaction is considered (Case 2), no size dependence is predicted from the resulting expression for γ, eq 11. Clearly, the uptake model does not describe our data adequately. Nonetheless, the functional form of the oleic acid decay given by eq 13 is useful for fitting the entire set of data and allows us to calculate the initial rate of decay and thus the value of γ at $t = 0$.

The most obvious explanation for the size dependence in γ_{meas} is that oleic acid diffusion within the particle is limiting the reaction and that the effect of this diffusion is more pronounced in the larger particles. The observed linear relationship will not hold in the limit of large particles since γ_{meas} cannot decrease below zero. Likewise, this size dependence cannot hold for sufficiently small particles since the rate of reaction will not be limited by diffusion and γ_{meas} will be constant with particle size. In fact, the spherical geometry of the particles can result in values of γ_{meas} that decrease with decreasing particle size when a/ℓ is small enough that the $(\coth(a/\ell) - \ell/a)$ term in eq 4 is less than unity. Thus, a more general approach to the solution of simultaneous reaction and diffusion must be taken to describe uptake over a range of particle sizes and experimental conditions.

Uptake Model Including Oleic Acid Diffusion. We believe that the observed decrease in γ_{meas} with particle radius is the result of oleic acid diffusion limiting the kinetics of the reaction. The oleic acid is not able to diffuse to the reaction region near the surface fast enough to maintain a uniform oleic acid concentration throughout the particle. The larger the particle, the farther the oleic acid must diffuse, hence the decrease in reactive uptake as the particle size increases.

Explicitly including the effect of oleic acid diffusion results in a set of coupled partial-differential equations in both $[O_3]$ and [Oleic]:

$$\frac{\partial[O_3]}{\partial t} = D\nabla^2[O_3] - k_2[O_3][\text{Oleic}] \quad (15)$$

$$\frac{\partial[\text{Oleic}]}{\partial t} = D'\nabla^2[\text{Oleic}] - k_2[O_3][\text{Oleic}] \quad (16)$$

where both $[O_3]$ and [Oleic] are functions of time and position. It is not possible to obtain analytical solutions to this set of partial differential equations, but with values of D, k_2, H, P_{O_3}, a, and D' (the oleic acid diffusion constant), solutions for $[O_3]$ and [Oleic] can be obtained numerically. This approach to solving eqs 15 and 16 does not rely on assuming that $[O_3]$ reaches a steady-state value or that oleic acid diffuses quickly throughout the particle. In fact, no functional form is assumed for either $[O_3]$ or [Oleic], and both concentrations are allowed to vary as functions of both position and time. A more detailed description of this procedure will be given in a forthcoming paper.[44]

To investigate the role of oleic acid diffusion in the reactive uptake of O_3, we obtain solutions numerically for [Oleic] using the differential equation solver in Mathematica (version 4.1, Wolfram Research). The values of the radius, a, and the O_3 partial pressure, P_{O_3}, were chosen to match those used in the experiments. The other parameters used are representative of the O_3−oleic acid system: $D = 1 \times 10^{-5}$ cm^2 s^{-1}, $H = 0.48$ M atm^{-1}, and $k_2 = 1 \times 10^6$ M^{-1} s^{-1},[41] where the value for D is an approximation based on measured diffusion constants for O_2 in organic solvents.[40] The value for H is an estimate based on measured solubility constants for O_3 in a variety of organic solvents[45,46] and has been adjusted slightly to yield an uptake coefficient of $\gamma_{meas} = 7.3 \times 10^{-3}$ that is consistent with our estimate of $\gamma_{meas} = (5.8-9.8) \times 10^{-3}$ for small particles for which oleic acid diffusion is not limiting.

Using the self-diffusion constant of oleic acid, $D' = 3 \times 10^{-7}$ cm^2 s^{-1},[1] it was found that oleic acid is well-mixed in the particle and that the rate of reaction is not limited by oleic acid diffusion. Under these conditions the simple model presented earlier (Case 1b) is valid. However, as the reaction with O_3 proceeds, oleic acid will be replaced with products of the reaction, and these products may slow diffusion to the reaction region near the surface. Indeed, the numerical solutions obtained for [Oleic] can fit only the experimental data (Figure 7) with D' slowed to $(4-10) \times 10^{-10}$ cm^2 s^{-1} (depending on particle size). Since D' is necessarily large (the self-diffusion constant) at the beginning of the reaction and then is reduced due to the formation of products, the constant value of D' represents an "effective" diffusion constant, and its inclusion allows the model to describe the rate of reactive uptake more accurately. By choosing realistic values for H, D, and k_2 (with a and P_{O_3} reflecting the conditions of each experiment), we can fit all of our data with reduced values of D', indicating that oleic acid diffusion is limiting and that the observed size dependence in γ_{meas} can be attributed to slow diffusion of oleic acid.

It is possible that the slowing represented by the decrease in D' reflects a reduction in the solubility of O_3 in the particle as the reaction proceeds and not a change in the oleic acid diffusion. This change in solubility could affect the rate of uptake, but it would not result in an observed size dependence in γ_{meas}. Thus, we favor the explanation based on the decrease in the rate of oleic acid diffusion. One explanation for this large decrease in D' is that the ozonolysis reaction initiates polymerization, which effectively inhibits diffusion of oleic acid. Indeed, we have observed a similar, but even more drastic, effect on the rate of reactive uptake in the ozonolysis of 1-octadecene

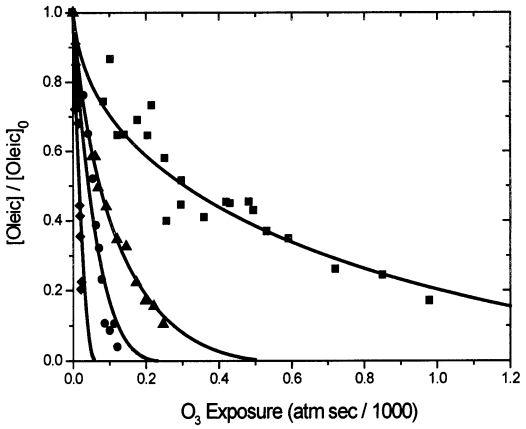

Figure 7. Numerical fits to the measured oleic acid decay profiles for four particle sizes: ◆ 680 nm, ● 1.38 μm, ▲ 1.86 μm, ■ 2.45 μm. The decays are fit with the diffusion-reaction model using the following parameters: $H = 0.48$ M atm^{-1}, $k_2 = 1 \times 10^6$ M^{-1} s^{-1}, $D = 1 \times 10^{-5}$ cm^2 s^{-1} The value of D' is allowed to vary for each particle size, with D' ranging from 4×10^{-10} cm^2 s^{-1} to 10×10^{-10} cm^2 s^{-1}.

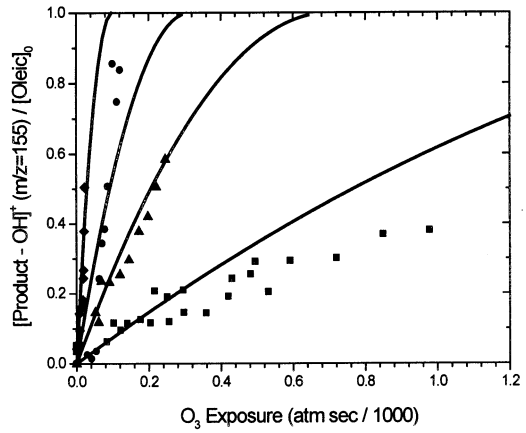

Figure 8. Rise of peak at $m/z = 155$ as a function of O_3 exposure ($P_{O_3}t$) for four particle sizes: ◆ 680 nm, ● 1.38 μm, ▲ 1.86 μm, ■ 2.45 μm. Lines represent expected signal if every oleic acid molecule that reacts results in the creation of a fragment at $m/z = 155$.

where the reaction is completely quenched after only 30% of the particle has reacted.[47]

All of the parameters, including H, P_{O_3}, k_2, a, D, and D', are coupled in determining the rate of uptake, and no simple expression for γ can be formulated. For example, D' becomes more significant as $[O_3]$ increases in the particle (and thus H and P_{O_3}) or as the particle size, a, increases. Additionally, since the rate of diffusion of oleic acid is likely changing as the reaction products are formed, treating D' as a constant does not necessarily describe the effect of diffusion accurately. The most general approach accounting for these coupled processes and the changing environment within the particle is the numerical solution to the coupled diffusion-reaction equations (15) and (16), and in future work we will address the general relationship between all of the relevant parameters.[44]

Product Kinetics. In this study the appearance of one of the products is also monitored as a function of O_3 exposure. The rise in signal of the feature at $m/z = 155$, perhaps a fragment of the ozonolysis product 9-oxononanoic acid, is shown in Figure 8 for each of the four particle sizes used in these experiments. The signals have been normalized to the initial oleic acid signal (at $m/z = 282$), assuming equal detection efficiency for the peaks at $m/z = 155$ and $m/z = 282$, and the corresponding solid curves are calculated from the measured

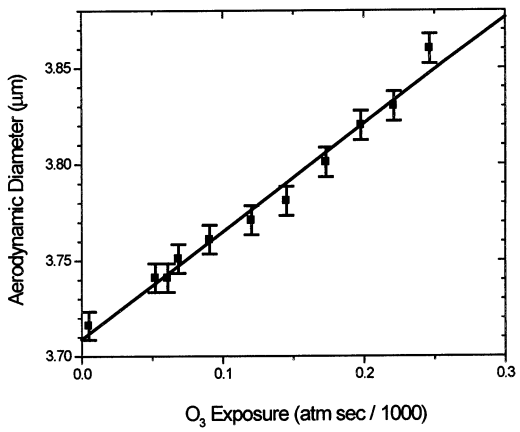

Figure 9. Growth of aerodynamic diameter of particles as a function of the extent of reaction. An estimate of 3.9×10^{-3} is calculated for γ_{meas} from the size increase (compared to a value of 3.1×10^{-3} calculated from the oleic acid decay data in Figure 5).

oleic acid decay rates. The similarity in the calculated and measured rises indicates a branching ratio of near unity for the peak at $m/z = 155$. This peak may not represent a fragment of the 9-oxononanoic acid product because this is only one of two product pathways expected to be possible (see Figure 8), and therefore the branching ratio should be less than unity. The peak may also represent a fragment of a secondary ozonide, in which case the branching ratio could be close to unity. However, a more definitive interpretation of these kinetics and the implications for the rates of product formation is not possible without more complete information regarding all of the products as well as the rate of unimolecular dissociation of the primary ozonide.

Particle Growth. As O_3 reacts with the oleic acid particles, it is incorporated into the particle through the creation of ozonolysis products. This incorporation leads to a net increase in the mass of the particle as long as the products do not evaporate. If the density of the particle were to remain constant, this mass increase would result in an increase in the volume, and thus diameter. The increase in the aerodynamic diameter of the particle, which is proportional to the geometric diameter and the square root of the density, can be measured with laser velocimetry as the reaction proceeds. Indeed, the aerodynamic diameters of the particles are seen to increase with exposure to O_3, as shown in Figure 9. Here, pure oleic acid particles 3.72 μm in diameter grow linearly in size to a diameter of 3.86 μm. By assuming no change in the density of the particle, we can calculate a value of $\gamma_{meas} = 3.9 \times 10^{-3}$ from the measured rate of mass uptake. This value is in good agreement with the uptake ($\gamma_{meas} = 3.1 \times 10^{-3}$) that we measured independently from the rate of oleic acid decay for the same particle size. Changes in particle radius as small as 3 nm are detectable with this method and provide an alternative diagnostic of the extent of reaction in the particle.

Discussion

Comparison to Other Studies. Two other groups have recently studied the uptake of O_3 by oleic acid and their experiments offer useful comparisons to our measurements. The work of Worsnop and co-workers[17] is similar to ours in that the composition of oleic acid particles reacted with O_3 was monitored with an aerosol mass spectrometer. However, their particles were smaller than ours, ranging in radius from 100 to 300 nm. The reported uptake coefficient of $(1.6 \pm 0.2) \times 10^{-3}$ (for all sizes) is significantly smaller than our value of $\gamma_{meas} = (7.3 \pm 1.5) \times 10^{-3}$ for our smallest particle, 680 nm in radius. A possible explanation for this discrepancy is that the signal monitored by Worsnop and co-workers included peaks other than $m/z = 282$. In their mass spectrum, the peak near $m/z = 282$ appears to shift to a smaller mass-to-charge ratio upon reaction with O_3, and with insufficient resolution or digitization integration of this signal could lead to an overestimation of the oleic acid concentration and thus an underestimation in the rate of uptake and in γ. Nonetheless, the lack of a size dependence in their values of γ confirms our expectation that the diffusion of oleic acid does not limit the rate of reaction for sufficiently small particles.

Recently, Moise, and Rudich[27] have also measured the rate of uptake of O_3 by oleic acid in a coated-wall flow tube study. By monitoring the rate of change of the concentration of O_3 in the gas phase, they were able to calculate a value of $\gamma = (8.3 \pm 0.9) \times 10^{-4}$, also significantly smaller than our value of γ for particles not limited by oleic acid diffusion. It is likely that this discrepancy results from the fact that the oleic acid coatings in their flow tube study are much thicker than our particles. The thick coatings result in a smaller uptake because oleic acid diffusion to the region near the surface is more acutely inhibited.

Atmospheric Implications. Individual particles found in the atmosphere often contain many different species including alkanes, alkenes, alcohols, and carboxylic acids. The rate at which these particles react with gases such as O_3 will depend on the composition of the particle as well as the rate of reaction of O_3 with each of the component species. With a value of $\gamma = 7 \times 10^{-3}$ and $[O_3] = 100$ ppb, 99% of a 50 nm particle of pure oleic acid would react in less than two minutes. However, the oleic acid concentration measured in atmospheric particles[10] suggests that oleic acid in aerosols has a much longer lifetime.

This apparent discrepancy could be attributed to the diffusion of oleic acid. The calculation assumes that oleic acid diffusion within the particle is fast and therefore does not limit the uptake. However, we have seen that under conditions in which the oleic acid diffusion is significantly reduced (compared to self-diffusion), uptake is much slower. Therefore, particle morphology, as well as composition, can play a role in the uptake of a gas-phase species. If oleic acid exists in a particle with other species that effectively inhibit diffusion within the particle, uptake will be reduced. Additionally, the location of the oleic acid within each particle could affect uptake, since oleic acid near the surface reacts much more quickly than it would if it were deep within the particle. Also, a particle with a very porous structure may inhibit the reaction more than a liquid droplet, for example, and therefore reduce O_3 uptake.

In addition to affecting the composition and properties of particles in the atmosphere, the reaction of O_3 with organic particle constituents may also affect the lifetime of O_3 in the troposphere.[16] The rate at which an aerosol removes a gas-phase species through reactive uptake can be estimated. Again, using a value of $\gamma = 7.3 \times 10^{-3}$ and a representative organic aerosol content of 1.5×10^5 particles cm^{-3} (for an urban setting[48]) with a radius of 25 nm and an average oleic acid content of 1%, this rate is calculated to be 8×10^{-6} s^{-1}, corresponding to an O_3 lifetime (with respect to reaction with the aerosol) of 36 h. The lifetime with respect to photochemical loss, for comparison, varies from a couple of days to a few hundred days depending on season and latitude.[49] Thus, organic species, such as oleic acid, residing in particles could have an impact on the atmospheric lifetime of O_3.

Conclusion

The reactive uptake of O_3 by oleic acid particles has been measured using a single-particle mass spectrometer to monitor

the composition of the aerosol as it reacts. The measured uptake coefficients display a size dependence, with γ_{meas} ranging from $(0.99 \pm 0.09) \times 10^{-3}$ for particles of radius 2.45 μm to $(7.3 \pm 1.5) \times 10^{-3}$ for particles of radius 680 nm. Numerical solutions of the coupled partial differential equations describing the simultaneous diffusion and reaction of both O_3 and oleic acid indicate that slow oleic acid diffusion can account for the observed size dependence in γ_{meas}. An approach that couples all processes relevant to uptake must be used to accurately describe the overall rate of uptake which is represented by γ. In particular, it is necessary to account for the interdependence of reaction and diffusion within the particle, not included in the conventional electric circuit resistance model. Finally, these experiments indicate that morphology, in addition to composition, may determine the reactivity of particles in the troposphere.

Acknowledgment. We gratefully acknowledge support from AFOSR, Grant F496020-99-1-0064, NSF, Grant CHE 9727788, DARPA, Grant F496020-98-1-0268, and EPA, Grant R-826767-01-0. C.L.D. acknowledges support from the EPA STAR fellowship. We thank Dr. Doug Worsnop of Aerodyne Research, Inc., Dr. Yinon Rudich of the Weizmann Institute, and Dr. Paul Ziemann of UC-Riverside for providing us with unpublished results. We also thank Dr. Worsnop for numerous useful discussions regarding the mathematics of reactive uptake. Finally, we thank the two anonymous reviewers for many useful comments.

Appendix I

Making the common assumptions that: (1) $[O_3]$ is in steady state and (2) [Oleic] is uniform throughout the particle, the differential equation in $[O_3]$ (eq 3) can be simplified

$$D\nabla^2[O_3] = k[O_3] \tag{I.1}$$

Since the particles are spherically symmetric, this equation can be rewritten as

$$D\nabla^2[O_3] = \frac{D}{r^2}\left[\frac{\partial}{\partial r}\left(r^2\frac{\partial[O_3]}{\partial r}\right) + \frac{1}{\sin\theta}\frac{\partial}{\partial\theta}\left(\sin\theta\frac{\partial[O_3]}{\partial\theta}\right) + \frac{1}{\sin^2\theta}\frac{\partial^2[O_3]}{\partial\phi^2}\right] = k[O_3]$$

$$= \frac{D}{r^2}\frac{\partial}{\partial r}\left(r^2\frac{\partial[O_3]}{\partial r}\right) = k[O_3] \tag{I.2}$$

This equation has been simplified by utilizing the fact that $[O_3]$ is spherically symmetric and is only a function of the radial depth in the particle, i.e., $\partial[O_3]/\partial\theta = \partial^2[O_3]/\partial f^2 = 0$.

Equation I.2 can then be solved by a substitution of variables: $u = [O_3]r$ to yield

$$\frac{d^2u}{dr^2} = \frac{u}{\ell^2} \tag{I.3}$$

$$u(r) = A\cosh(r/\ell) + B\sinh(r/\ell) \tag{I.4}$$

$$[O_3](r) = \frac{u(r)}{r} = \frac{1}{r}[A\cosh(r/\ell) + B\sinh(r/\ell)] \tag{I.5}$$

where $\ell = (D/k)^{1/2}$ is the diffuso-reactive length.

Since $[O_3](0)$, the concentration of O_3 at the center of the particle, must be finite, $A = 0$. Additionally, $[O_3](a)$, the concentration of O_3 at the surface, is constant in time and is equal to the Henry's Law solubility value, HP_{O_3} (assuming that O_3 from the gas-phase replenishes the surface faster than the rate at which it reacts in the particle) which results in

$$[O_3](r) = HP_{O_3}\frac{a}{\sinh(a/\ell)}\frac{\sinh(r/\ell)}{r} \tag{I.6}$$

The flux of O_3 into the particle can be obtained from Fick's first law by calculating the $[O_3]$ gradient as the derivative of eq I.6

$$\frac{d[O_3]}{dr}\Big|_{r=a} = HP_{O_3}\frac{1}{a}[(a/\ell)\coth(a/\ell) - 1] \tag{I.7}$$

$$\text{flux}_{surf} = -D\left(-\frac{d[O_3]}{dr}\right)_{r=a} = P_{O_3}H\frac{D}{\ell}(\coth(a/\ell) - \ell/a) \tag{I.8}$$

Here, the negative of the $[O_3]$ gradient is used since it is the flux into the particle that is being calculated. An expression for the uptake coefficient, eq 4, is obtained by normalizing this flux to the O_3−particle collision rate

$$\Gamma_{rxn} = \frac{\text{flux}_{surf}}{P_{O_3}\bar{c}/4RT} = \frac{4HRT}{\bar{c}}\frac{D}{\ell}(\coth(a/\ell) - \ell/a) \tag{4}$$

Appendix II

Substitution of the expression for Γ_{rxn} (eq 4) for γ in the expression relating the rate of change of [Oleic] to γ (eq 1) yields a differential equation for [Oleic] in time

$$\frac{d[\text{Oleic}]}{dt} = -\gamma\left(\frac{P_{O_3}\bar{c}}{4RT}\right)\frac{S_A}{V} \tag{1}$$

$$\frac{d[\text{Oleic}]}{dt} = -3P_{O_3}H\frac{D}{a\ell}(\coth(a/\ell) - \ell/a)$$

$$= -\frac{3P_{O_3}H\sqrt{k_2D}}{a}\sqrt{[\text{Oleic}]}\times\left[\coth\left(a\sqrt{\frac{k_2[\text{Oleic}]}{D}}\right) - \frac{1}{a}\sqrt{\frac{D}{k_2[\text{Oleic}]}}\right] \tag{II.1}$$

Equation II.1 is the general differential equation for the concentration of oleic acid including the diffusion of O_3 within the particle and reaction with oleic acid in the bulk of the particle. A general analytical solution to this equation cannot be found. However, solutions can be found in certain limiting cases.

Case 1a: Rapid Diffusion of O_3 Throughout the Particle ($\ell > a$). In the limit that ℓ is larger than the radius of the particle (a), the $\coth(a/\ell)$ term in eq II.1 can be approximated by a Taylor expansion. In the following derivation, the substitution $x = a/\ell$ has been made, and the resulting expression, eq 7, is valid to within 6% when $a/\ell < 1$.

$$\coth\left(\frac{a}{\ell}\right) - \frac{\ell}{a} = \left(\frac{e^{x} + e^{-x}}{e^{x} - e^{-x}}\right) - \frac{1}{x} \tag{II.2}$$

$$= \frac{(x-1)e^{2x} + (x+1)}{x(e^{2x} - 1)} \tag{II.3}$$

$$= \frac{(x-1)\left(1 + 2x + \frac{(2x)^2}{2!} + \frac{(2x)^3}{3!} + \cdots\right) + (x+1)}{x\left(1 + 2x + \frac{(2x)^2}{2!} + \frac{(2x)^3}{3!} + \cdots - 1\right)} \tag{II.4}$$

$$\cong \frac{1}{3}x = \frac{1}{3}\frac{a}{\ell} \tag{II.5}$$

Substituting this approximation for the $[\coth(a/\ell) - \ell/a]$ term in eq II.1 reduces the equation to

$$\frac{d[\text{Oleic}]}{dt} \cong -P_{O_3}H\frac{D}{\ell^2} = -P_{O_3}Hk_2[\text{Oleic}] \tag{II.6}$$

Solving this differential equation yields

$$[\text{Oleic}] = [\text{Oleic}]_0 \exp(-P_{O_3}Hk_2t) \tag{6}$$

$$\gamma = \frac{4HRT}{\bar{c}}\frac{a}{3}k_2[\text{Oleic}] \tag{7}$$

Case 1b: Reaction Near the Surface of the Particle ($\ell < a/20$). In the limit that ℓ is much smaller than the radius of the particle (a), the $[\coth(a/\ell) - a/\ell]$ term in eq II.1 approaches an asymptotic value of 1. Approximating this term as 1 is valid to within 5% when $a/\ell > 20$, and eq II.1 can be simplified

$$\frac{d[\text{Oleic}]}{dt} \cong -3P_{O_3}H\frac{D}{a\ell} = -\frac{3P_{O_3}H\sqrt{Dk_2}}{a}\sqrt{[\text{Oleic}]} \tag{II.7}$$

Solving this differential equation yields

$$\sqrt{[\text{Oleic}]} = \sqrt{[\text{Oleic}]_0} - \frac{3P_{O_3}H\sqrt{Dk_2}}{2a}t \tag{8}$$

$$\gamma = \frac{4HRT}{\bar{c}}\sqrt{Dk_2}\sqrt{[\text{Oleic}]} \tag{9}$$

Case 2: Reaction at the Surface. Substituting Γ_{surf} (eq 11)

$$\Gamma_{surf} = \frac{-\frac{d[\text{Oleic}]_{surf}}{dt}}{P_{O_3}\bar{c}/4RT} = \frac{4HRT}{\bar{c}}\delta^2 k_2^{surf}[\text{Oleic}] \tag{11}$$

for γ in eq 1 yields

$$\frac{d[\text{Oleic}]}{dt} = -\frac{3\delta^2}{a}P_{O_3}Hk_2^{surf}[\text{Oleic}] \tag{II.8}$$

and solving this equation leads to an expression for [Oleic]

$$[\text{Oleic}] = [\text{Oleic}]_0 \exp\left(-\frac{3\delta^2}{a}P_{O_3}Hk_2^{surf}t\right) \tag{12}$$

References and Notes

(1) Iwahashi, M.; Kasahara, Y.; Matsuzawa, H.; Yagi, K.; Nomura, K.; Terauchi, H.; Ozaki, Y.; Suzuki, M. *J. Phys. Chem. B* **2000**, *104*, 6186−6194.

(2) Gill, P. S.; Graedel, T. E.; Weschler, C. J. *Rev. Geophys.* **1983**, *21*, 903−920.

(3) Murphy, D. M.; Thomson, D. S.; Mahoney, M. J. *Science* **1998**, *282*, 1664−1669.

(4) Simoneit, B. R. T.; Sheng, G.; Chen, X.; Fu, J.; Zhang, J.; Xu, Y. *Atmos. Environ.* **1991**, *25A*, 2111−2129.

(5) Graedel, T. E.; Hawkins, D. T.; Claxton, L. D. *Atmospheric Chemical Compounds: Sources, Occurrence, and Bioassay*; Academic Press: Orlando, 1986.

(6) Ketseridis, G.; Hahn, J.; Jaenicke, R.; Junge, C. *Atmos. Environ.* **1976**, *10*, 603−610.

(7) Finlayson-Pitts, B. J.; Pitts, J. N. *Chemistry of the Upper and Lower Atmosphere: Theory, Experiments and Applications*; Academic Press: New York, 2000.

(8) Simoneit, B. R. T. *J. Atmos. Chem.* **1989**, *8*, 251−275.

(9) Standley, L. J.; Simoneit, B. R. T. *Atmos. Environ.* **1990**, *24B*, 67−73.

(10) Rogge, W. F.; Hildemann, L. M.; Mazurek, M. A.; Cass, G. R.; Simoneit, B. R. T. *Environ. Sci. Technol.* **1991**, *25*, 1112−1119.

(11) Thomas, E. R.; Frost, G. J.; Rudich, Y. *J. Geophys. Res.* **2001**, *106*, 3045−3056.

(12) Paulson, S. E.; Orlando, J. J. *Geophys. Res. Lett.* **1996**, *23*, 3727−3730.

(13) Razumovskii, S. D.; Zaikov, G. E. *Ozone and its Reactions with Organic Compounds*, Elsevier: Amsterdam, 1984.

(14) Underwood, G. M.; Li, P.; Usher, C. R.; Grassian, V. H. *J. Phys. Chem. A* **2000**, *104*, 819−829.

(15) Hanson, D. R.; Burkholder, J. B.; Howard, C. J.; Ravishankara, A. R. *J. Phys. Chem.* **1992**, *96*, 4979−4985.

(16) deGouw, J. A.; Lovejoy, E. R. *Geophys. Res. Lett.* **1998**, *25*, 931−937.

(17) Morris, J. W.; Davidovits, P.; Jayne, J. T.; Shi, Q.; Kolb, C. E.; Worsnop, D. R.; Barney, W. S.; Jimenez, J.; Cass, G. R. *Geophys. Res. Lett.*, in press.

(18) Woods, E., III; Smith, G. D.; Dessiaterik, Y.; Baer, T.; Miller, R. E. *Anal. Chem.* **2001**, *73*, 2317−2322.

(19) Woods, E., III; Smith, G. D.; Miller, R. E.; Baer, T. *Anal. Chem.* **2002**, *74*, 1642−1649.

(20) Molina, L. T.; Molina, M. J. *J. Geophys. Res.* **1986**, *91*, 14501−14508.

(21) Liu, P.; Ziemann, P. J.; Kittelson, D. B.; McMurry, P. H. *Aerosol Sci. Technol.* **1995**, *22*, 293−313.

(22) Liu, P.; Ziemann, P. J.; Kittelson, D. B.; McMurry, P. H. *Aerosol Sci. Technol.* **1995**, *22*, 314−324.

(23) Schreiner, J.; Voigt, C.; Mauersberger, K.; McMurry, P. H.; Ziemann, P. J. *Aerosol Sci. Technol.* **1998**, *29*, 50−56.

(24) Tobias, H. J.; Ziemann, P. J. *J. Phys. Chem. B* **2001**, *105*, 6129−6135.

(25) Paulson, S. E.; Chung, M. Y.; Hasson, A. S. *J. Phys. Chem. A* **1999**, *103*, 8125−8138.

(26) Ziemann, P. J., personal communication, 2002.

(27) Rudich, Y., personal communication, 2002.

(28) *NIST Chemistry WebBook, NIST Standard Reference Database Number 69*, February 2000 ed.; National Institute of Standards and Technology: Gaithersburg, MD, 2001.

(29) Nathanson, G. M.; Davidovits, P.; Worsnop, D. R.; Kolb, C. E. *J. Phys. Chem.* **1996**, *100*, 13007−13013.

(30) Kolb C. E.; Worsnop, D. R.; Zahniser, M. S.; Davidovits, P.; Keyser, T. R.; Leu, M. T.; Molina, M. J.; Hanson, D. R.; Ravishankara, A. R. *Progress and Problems in Atmospheric Chemistry: Current Problems in Atmospheric Chemistry*; 1995; pp 771−875.

(31) Danckwerts, P. V. *Trans. Faraday Soc.* **1950**, *46*, 300−304.

(32) Danckwerts, P. V. *Trans. Faraday Soc.* **1951**, *47*, 1014−1023.

(33) Danckwerts P. V. *Gas−Liquid Reactions*; McGraw-Hill: New York, 1970; Chapter 3, pp 30−70.

(34) Schwartz, S. E.; Freiberg, J. E. *Atmos. Environ.* **1981**, *15*, 1129−1144.

(35) Hanson, D. R. *J. Phys. Chem. B* **1997**, *101*, 4998−5001.

(36) Hu, J. H.; Shi, Q.; Davidovits, P.; Worsnop, D. R.; Zahniser, M. S.; Kolb, C. E. *J. Phys. Chem.* **1995**, *99*, 8768−8776.

(37) Hanson, D. R.; Ravishankara, A. R.; Solomon, S. *J. Geophys. Res.* **1994**, *99*, 3615−3629.

(38) Shi, Q.; Davidovits, P.; Jayne, J. T.; Worsnop, D. R.; Kolb, C. E. *J. Phys. Chem. A* **1999**, *103*, 8812−8823.

(39) Gershenzon, M.; Davidovits, P.; Jayne, J. T.; Kolb, C. E.; Worsnop, D. R. *J. Phys. Chem. A* **2000**, *105*, 7031−7036.

(40) *Handbook of Physical Quantities*; CRC Press: Boca Raton, 1997; pp 476−478.

(41) Razumovskii, S. D.; Zaikov, G. E. *Z. Organich. Khim.* **1972**, *8*, 468−472.
(42) *CRC Handbook of Chemistry and Physics*, 81st ed.; Lide, D. R., Ed.; CRC Press: Boca Raton, 2000.
(43) Worsnop, D. R.; Morris, J. W.; Shi, Q.; Davidovits, P.; Kolb, C. E. *Geophys. Res. Lett.*, submitted.
(44) Smith, G.; Woods, E., III; Baer, T.; Miller, R. E., in preparation.
(45) Razumovskii, S. D.; Zaikov, G. E. *Bull. Acad. Sci. USSR, Div. Geologic* **1971**, 616−620.
(46) Tarunin, B. I.; Perepletchikov, M. L.; Aleksandrov, Y. A. *Z. Obsch. Khim. (English)* **1982**, *52*, 419−422.
(47) Smith, G. D.; Woods, E., III; Baer, T.; Miller, R. E., in preparation.
(48) Heintzenberg, J. *Tellus* **1989**, *41B*, 149−160.
(49) Liu, S. C.; Trainer, M. *J. Atmos. Chem.* **1988**, *6*, 221−233.